International Journal of Microwave and Wireless Technologies, 2009, 1(1), 19–27.
doi:10.1017/S1759078709000038 Printed in the United Kingdom

Piezoelectric materials parameters for piezoelectric thin films in GHz applications

P. MURALT[1], J. CONDE[1], A. ARTIEDA[1], F. MARTIN[1] AND M. CANTONI[2]

Piezoelectric thin films have existing and promising new applications in microwave filter technologies. The final performance depends on many parameters, and very specifically on the materials properties of each involved material. In this article, materials and properties for thin-film bulk acoustic wave resonators are discussed on some selected issues: the piezoelectric coefficients and acoustic losses of AlN, the relation of the first one with microstructural parameters, the inclusion of parasitic elements, and the merits of and problems with ferroelectric materials.

Keywords: Aluminum nitride, Ferroelectrics, Bulk acoustic waves, Thin films

Received 15 July 2008; Revised 27 October 2008

I. INTRODUCTION

The wurtzite materials AlN and ZnO are currently the only piezoelectrics that are used in thin-film form for microwave applications in the 1–10 GHz range. They combine good piezoelectric properties with excellent acoustic qualities, and grow most easily in the optimal film orientation for RF filter applications. In addition, they can be synthesized by sputter deposition, a plasma method allowing for low processing temperatures. According to Hickernell [1], efforts to grow ZnO thin films go back to around 1965; good-quality films were obtained in the mid- to late 1970s, mostly by sputtering [2, 3], but also by CVD [4]. Besides electro-acoustic applications, optical applications [4] were also investigated. The potential of these films for RF filtering with bulk acoustic waves (BAWs) was soon discovered [5–7]. Such devices are composed of several electromechanical resonators, commonly called thin-film bulk acoustic resonators (TFBARs), which are based on standing bulk waves trapped in a film slab, as sketched in Fig. 1, whereby film thickness defines the frequency of resonance. In these early years, ZnO was much more frequently investigated than AlN. Insufficient vacuum in the deposition tools at this time is certainly one of the reasons, because nitrides require much better vacuum conditions than oxides. In addition, the target applications had frequencies in the ultra-high frequency range (television), requiring a film thickness of several micrometers. This is not ideal for a material such as AlN that tends to create immense mechanical stresses, and also exhibits a very high sound velocity requiring almost twice as thick layers as with ZnO. Anyhow, the time was not yet ripe for TFBARs. Surface acoustic wave (SAW) devices based on piezoelectric single crystals such as quartz, $LiNbO_3$, and $LiTaO_3$ were and are much more practical in the frequency range below 1 GHz. SAW filter production was much less demanding, once single-crystal wafers of these materials were available. TFBARs had to wait until the mid-1990s for the first industrial activities [8, 9]. Sputter sources and industrial-type vacuum systems were considerably improved in the meantime, MEMS technology was already at a suitable development stage, and then the application was ready as well: mobile communication. Especially the second generation with carrier frequencies around 2 GHz was and still is ideal for TFBARs, because the required thin-film thickness is in a reasonable range. After the year 2000, TFBAR filters for mobile phones entered industrial production on a larger scale, first as membrane structures [10] and later also with acoustic reflectors [11, 12]. BAW filters are especially suited to obtain passbands with very sharp drops to large rejection at the band edge, as is possible with the so-called ladder filter design. This is the desired property for duplex filters. They provide RF filtering on the Rx and Tx bands, while keeping a minimal frequency separation between the bands. Today, AlN is in most, or even in all, cases the preferred material for TFBARs. The first reason is that the relevant properties of AlN are sufficient to reach specifications for RF filters in mobile telecommunication. In addition, AlN can handle higher power levels than ZnO because its thermal conductivity is larger and its dielectric losses are lower. Furthermore, its chemical composition complies with semiconductor fabrication requirements, and thus constitutes the ideal material for above-IC integration. First, above-IC integration of AlN FBAR filters has been successfully demonstrated in planar integration on GaAs devices [13], and more recently in vertical integration above Si ICs [14].

TFBARs exploit the fundamental, thickness extensional mode of a piezoelectric plate that is much wider than thick, as schematically drawn in Fig. 1. The amplitude of this mode points along the *z*-direction. The strains in the layer plane are zero [15], because lateral displacements cannot follow the thickness vibration. The relation between materials properties, microstructures, dimensions, and final properties is quite complex. Nonetheless, it has always been a major goal of device development to understand the underlying microstructure–property relations of the involved materials [1], and to characterize as much as possible on the level of

[1]Ceramics Laboratory, Ecole Polytechnique Federale de Lausanne EPFL, Lausanne, Switzerland
[2]Electron Microscopy Center, Ecole Polytechnique Federale de Lausanne EPFL, Switzerland.
Corresponding author:
P. Muralt
Email: paul.muralt@epfl.ch

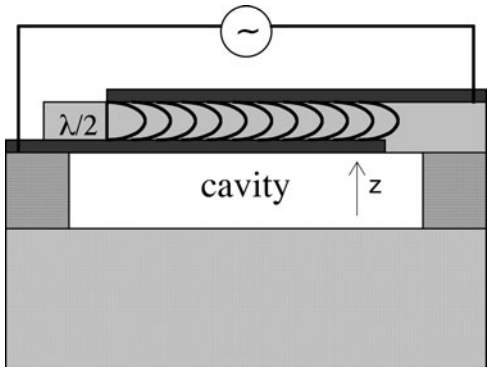

Fig. 1. Schematic drawing of a bulk acoustic resonance in a piezoelectric plate. The vertical dimension is very exaggerated. In the vibrating, active zone, the pressure amplitude for the fundamental mode is sketched. The trapped wave has half the wavelength within the slab thickness.

single layers in order to be able to predict device properties of the actual multilayer resonators. Of course, nothing can replace the evaluation of resonators. Only these can finally yield the correct coupling constants and quality factors. It is however important for research and development to apprehend specific features of process–microstructure relations that are important for properties. This advances the understanding of basic mechanisms that eventually can be generalized. In addition, it is useful to dispose of measurement techniques that allow the assessment of properties before full device fabrication. The motivation for further research in this area arises from the need to improve the current performance of RF filters. Even relatively small improvements in coupling and quality factor might be paying in terms of filter characteristics and commercial success. In addition, there are further ideas for applications, for instance in the direction of microwave oscillators [16, 17]. In their case, high-quality factors and temperature stability are crucial parameters. A very actual topicis the search for tuning possibilities. The tuning of frequencies could allow for a reduction in the number of filters in mobile phones.

In the following, some issues in the characterization of TFBARs and their materials are discussed. AlN is discussed in more detail while trying to find an answer to the question of how good AlN really is. This question is related to optimal substrates and microstructures. Later, the case of ferroelectrics is briefly presented, interesting for tunable filters. In this case, the control of microstructure in the large sense is very important.

II. PROPERTIES OF ALN AND ZNO

The two materials properties of primary interest in making wide band filters are coupling factor k_t^2 – defining the elastic energy stored in the plate for a given input electrical energy – and quality factor Q_m of the piezoelectric and further involved materials. The effective values obtained from a resonator characteristic depend on other features of the device, such as electrode properties.

For optimal coupling in a parallel plate capacitor, the polar c-axis of wurtzite structures must be grown perpendicular to the device plane, i.e. along z in Fig. 1. The piezoelectric coupling is then expressed in terms of material properties as:

$$k_t^2 = \frac{e_{33}^2}{c_{33}^D \varepsilon_0 \varepsilon_{33}^S} = \frac{e_{33}^2}{c_{33}^E \varepsilon_0 \varepsilon_{33}^T}, \quad (1)$$

where e_{33}, c_{33}^E, and ε_{33}^S are piezoelectric coefficient, stiffness at constant electric field (E) (or at constant displacement field D), and relative permittivity at constant strain S (or at constant stress T), respectively.

The quality factor of materials is limited by viscous losses [18]. The elastic constants have an imaginary part proportional to viscosity η, with the same tensorial properties as stiffness:

$$c_{33}^{D*} = c_{33}^D + i\omega\eta_{33}^D = c_{33}^D(1 + i\omega\tau_1). \quad (2)$$

A time constant τ_1 can be defined as $\tau_1 = \eta/c$, using the relevant stiffness constants c for the vibration mode in question, and the quality factor is then written as:

$$Q_m = \frac{1}{\omega\tau_1}. \quad (3)$$

The product $k_t^2 Q_m$ is introduced as a figure of merit for optimal resonator characteristics. (The ratio of the maximal to the minimal peak values of the impedance $|Z|$ is proportional to k^2Q of the resonator.) Using standard literature values for AlN and ZnO, the values for k_t^2 and Q_m are obtained as given in Table 1. This table shows that ZnO and AlN are approximately equivalent in terms of k^2Q. In practice, this figure of merit amounts to 50 to 100 rather than to 160. The table thus suggests that improvements are still possible. Other criteria may, however, become very important as well. Filters in the transmission line must survive high power densities. It turns out that AlN can withstand larger voltages without break-down, and exhibits lower leakage currents than ZnO. In addition, AlN is a better heat conductor than ZnO. All these properties contribute to better power handling with AlN resonators.

III. IS PERFORMANCE OF ALN BETTER THAN EXPECTED? PREDICTIONS FROM MICROSTRUCTURE–PROPERTY RELATIONS

Our knowledge on the piezoelectric properties of pure AlN stems mainly from thin films. There are no single-crystal reference data for the simple reason that the growth of perfect single crystals has not been mastered yet. The measured piezoelectric properties of crystals do not reach

Table 1. Relevant materials parameters for TFBAR applications for the two most used wurtzite thin films, as derived from standard literature data [18, 19].

	k_t^2 (%)	τ_1 (fs)	Q_m at 2 GHz	$k_t^2\,Q_m$ at 2 GHz
AlN	6.5	32	2490	160
ZnO	9	45	1770	160

Table 2. Materials constants of AlN from different sources. Standard data from epitaxial films on sapphire are compared to ab initio calculations and data from polycrystalline thin films (bold: primary data; italics: derived data).

	e_{33} (C/m²)	e_{31} (C/m²)	d_{33} (pm/V)	d_{31} (pm/V)	c_{33}^E (GPa)	c_{13}^E (GPa)	c_{11}^E (GPa)	c_{12}^E (GPa)	ε_{33} $\varepsilon_{33,f}$	$d_{33,f}$ (pm/V)	$e_{31,f}$ (C/m²)	k_t^2 (%)
Epi AlN/sapphire [25]	**1.55**	**− 0.58**	*5.53*	*− 2.65*	**395**	**120**	**345**	**125**	**9.5**	*3.92*	*1.37*	*6.5*
Ab initio [23]	*2.0*	*− 0.47*	**6.72**	**− 2.71**	395	120	345	125				
AlN/Pt [22, 26]	*2.0*	*− 0.68*	*7.0*	*− 3.2*	395	120			**10.2**	**5.1**	**1.3**	*11*
Resonators [24]	*1.67*											**7.8**

those of thin films [20]. For a long time, properties evaluated at SAW structures of epitaxial single crystalline films grown at high temperature served as standard values [21]. Recent work indicates that the piezoelectric coefficients are probably larger. A discrepancy exists especially with thin-film piezoelectric measurements based on interferometric techniques [22]. These measure the so-called clamped piezoelectric coefficient:

$$d_{33,f} = e_{33}/c_{33}^E. \tag{4}$$

Likewise, one usually measures an "unclamped" transverse coefficient $e_{31,f}$, unclamped because the film is free to move along the vertical direction z, perpendicular to the film plane (crystal direction three as well):

$$e_{31,f} = e_{31} - e_{33} \cdot c_{13}^E/c_{33}^E. \tag{5}$$

In Table 2, standard values are compared with recently published results from ab initio calculations [23], direct measurements of piezoelectric coefficients of polycrystalline textured films [22] (see Fig. 4), and coupling coefficient measurements of resonators of similar films [24]. These recent works strongly suggest that the piezoelectric coefficients of thin films are larger than expected to date. The $d_{33,f}$ value for very narrow rocking curve widths is extrapolated as 6.8 pm/V. This corresponds to k_t^2 values of 8–9%. This value agrees very well with the extrapolated k_t^2 of Löbl *et al.* [24], where the coupling is depicted as a function of rocking curve width.

The high-quality performance of polycrystalline thin films is not at all evident, given the polycrystalline microstructure (Fig. 2). However, the grains are very crystalline and oriented, as shown by the transmission electron microscopy (TEM) image and corresponding diffraction patterns (Fig. 3). In case of Pt (111) electrodes with their hexagonal (111) surface planes, the hexagonal AlN structure tends to nucleate epitaxially on each Pt grain, thereby promoting (001) growth of AlN. However, this mechanism is not necessary to achieve (001) growth. This orientation can also be obtained on amorphous substrates. The crucial process parameter is rather the energy of bombarding positive ions originating from the sputter plasma [27]. There is interesting evidence from different deposition methods that (001) growth is promoted by ion bombardment of energies in the range 20–40 eV, as evidenced by arc deposition [28] and RF sputtering [29]. However, it is not precisely known what this bombardment is effectively doing on the level of atoms, apart from promoting surface diffusion.

Usually, rocking curve width is interpreted in terms of tilted c-planes. This tilt would then directly result from the roughness of the substrate, given that the first atomic plane of a nucleus is defined by substrate surface. The tilt by a few degrees cannot explain, however, why the piezoelectric effect should be reduced so drastically. For small tilt angles α, the piezoelectric coefficient e_{33} should vary as:

$$\begin{aligned} e_{33}(\alpha) &= e_{33}^0 - \left\{\frac{3}{2}e_{33}^0 - e_{31}^0 + 2e_{15}^0\right\}\alpha^2 + O(\alpha^4) \\ &\approx e_{33}^0(1 - 0.42\alpha^2). \end{aligned} \tag{6}$$

The upper index o indicates the standard piezoelectric coefficients with no tilt between E-field and c-axis. The values of the e-coefficients were taken from ref. [19]. This effect should not even be visible on the value scale of Fig. 4. The discrepancy was also raised for a similar investigation dealing with the d_{31} coefficient of ZnO films in beam structures [30]. The reason is thus completely different. A further argument against a direct relation of tilt and polar ordering is the fact that the growth of piezoelectric AlN with a homogeneously tilted c-axis is possible [31–33], in spite of tilt angles being much larger than 5°. The direction of the polar axis matters, quite obviously. The sign of piezoelectricity is linked to the direction of this axis, meaning that we should make the difference between (0, 0, +1) and (0, 0, −1) orientations. A 1:1 mixture of these orientations yields zero piezoelectric effect. The mechanism that is responsible for the polarity choice is not well understood for low-temperature growth by sputtering. In high temperatures, for instance on sapphire at 900–1000°C, the orientation is certainly imposed by interface

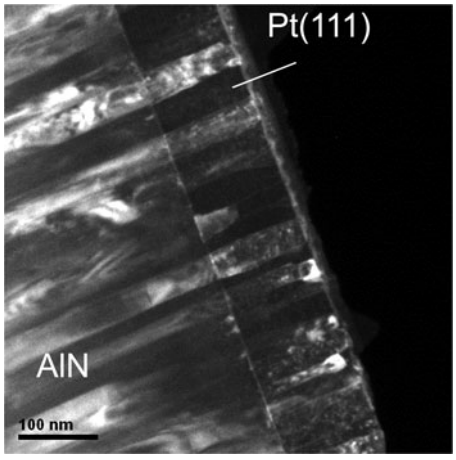

Fig. 2. Dark-field TEM image showing an AlN(001) thin film on a Pt(111) electrode. The epitaxial growth on single Pt grains is well visible (film as described in ref. [22]).

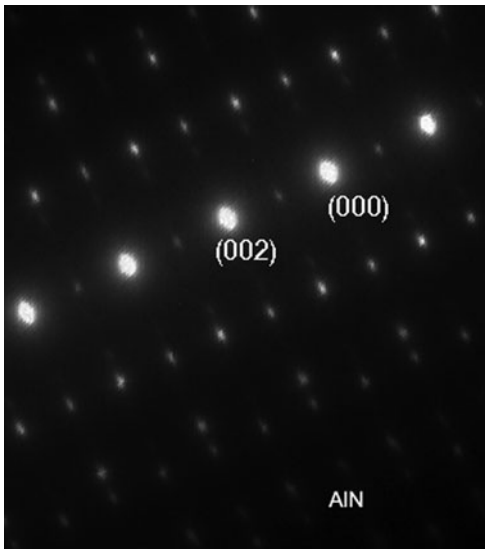

Fig. 3. TEM diffraction at the same AlN film as shown in Fig. 2. The diffraction pattern does not show any orientation other than (001).

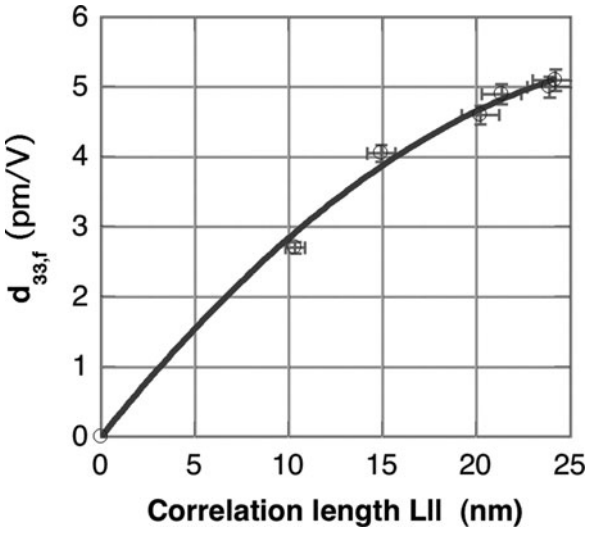

Fig. 5. Same data as in Fig. 4. This time, $d_{33,f}$ is displayed as a function of the in-plane coherence length according to the modified Scherrer equation (see [34, 35]) $L_{//} = 0.94\lambda/(\Delta\omega \sin \theta)$, where θ means the diffraction angle, $\Delta\omega$ the rocking curve width, and λ the X-ray wavelength.

and surface energies that are advantageous for one of the polarities.

This effect cannot be the only mechanism at low temperatures. Ion bombardment and further plasma impacts (there is also electron bombardment) certainly play a role in polarity choice, because the energy of bombarding ions plays a role.

There is also evidence that substrate chemistry may play a role. Ruffner *et al.* [36] found an influence of Ru electrode preparation, i.e. the degree of oxidation of Ru that leads to values ranging from -3.5 to $+4$ pm/V. The correlation with rocking curve widths would mean that the more perfect the growth approaches a kind of one-dimensional single-crystal growth with very extended *c*-planes, the better the relatively weak effect of mobility enhancement by plasma impact is able to promote one of the two polarities. Accordingly, one should interpret the rocking curve width as a correlation length issue rather than as a tilt issue. This is shown in Fig. 5, where $d_{33,f}$ is plotted against the correlation $L_{//}$, with the same data points as in Fig. 4. This figure suggests that there is an asymptotic value of around 6 pm/V that is approached for large correlation lengths, and that the curve might well start at zero for very thin AlN films of a few atomic layers. Thicker films show a larger correlation length. The values of $L_{//}$ correspond not too badly with the fiber-grain diameter, and thus with the in-plane grain boundary distance (see Fig. 3). In heteroepitaxial AlN on diamond, the correlation length was found to be about twice as large, i.e. 50 nm [35].

IV. DERIVATION OF MATERIALS PARAMETERS FROM RESONATORS

The English say that the proof of the pudding lies in its eating. One can argue analogously about materials qualities in an electro-acoustic device. Only the admittance or impedance curve tells us finally how good or bad the device as a whole is. Especially material quality factors can only be assessed by means of resonators. The problem is that several materials contribute with their losses. Resistive losses in electrodes become visible as well as acoustic losses in a gold electrode, for instance. There are thus a number of impacts we can assign to parasitic elements in the circuit. Resistive losses can be estimated from known metal conductivities, and by

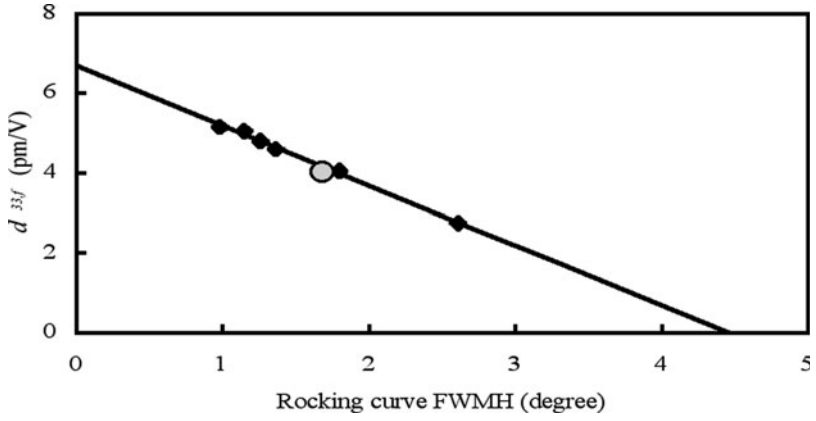

Fig. 4. Longitudinal piezoelectric coefficient $d_{33,f}$ as derived from interferometric measurements as a function of the rocking curve width of AlN thin films (from [22]). The varied process parameter was the deposition time, i.e. film thickness. Thicker films show a higher $d_{33,f}$.

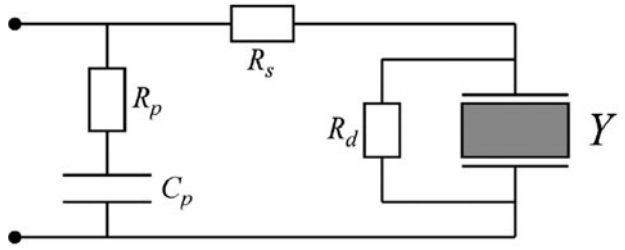

Fig. 6. Complete resonator model with series and parallel resistors R_s and R_p, a parallel capacitance C_p, and a parallel resistance R_d corresponding to dielectric losses. The resonator Y corresponds to the 2D finite-element model (from ref. [17]).

varying device geometries that change these losses in a defined way. The total circuit can be devised into a pure acoustic resonator (with admittance Y in Fig. 6) and parasitic elements. In the example shown in Fig. 6, these were mainly a series resistor R_s, a resistor taking care of dielectric losses R_d, and a resistance R_p originating from a slightly conductive substrate to which contact pads couple through a capacitor C_p. The admittance of the pure acoustic resonator can be calculated by means of finite-element modeling or suitable 1D analytical theories such as derived in ref. [37]. A knowledge of the parasitics allows finally for testing the performance if one could avoid the latter, and thus to access intrinsic materials parameters. Of course, one has to be careful and test several designs to see whether all the elements vary accordingly. An example for such work is given in Fig. 7. In this study, symmetric composite resonators of $SiO_2/AlN/SiO_2$ are sandwiched between electrodes in order to increase the quality factor and decrease the temperature coefficient [17]. The acoustic quality factor of SiO_2 should be about a factor of 3–6 better than that of AlN, if we rely on data collected for quartz [18, 38]. This is justified by the fact that the SiO_2 films are not doped with impurities known to degrade the Q-factor.

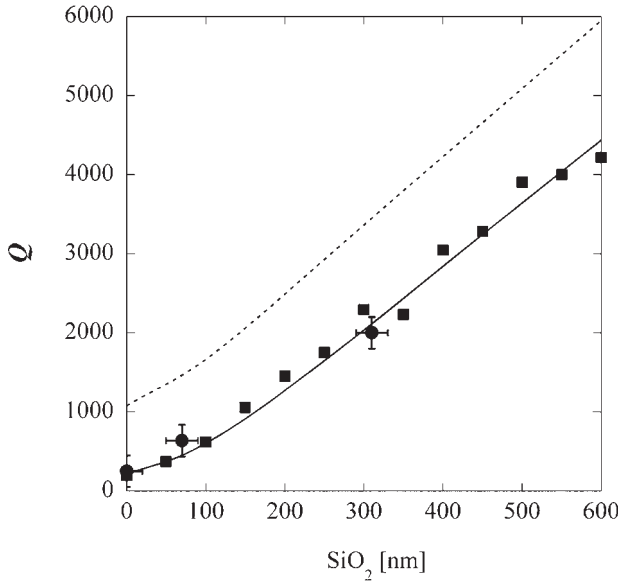

Fig. 7. TFBAR quality factor Q of a $SiO_2/AlN/SiO_2$ composite resonator. The dotted line predicts the resonator performance based on finite-element modeling including acoustic losses, but without resistive losses. The filled square marks correspond to FEM calculation including the parasitic elements (as in Fig. 6). The round dots are experimental data (from [17]).

V. FERROELECTRIC TFBARS

There are several motivations to seek new TFBAR materials. One is to avoid the large area and the large thickness needed for AlN resonators near 1 GHz (e.g. the GSM band). As the electrical impedance of the resonators is usually fixed by circuit and interconnect design, independently of frequency, the area of a resonator scales as

$$area \propto \frac{t_p}{\omega \cdot \varepsilon} \propto \frac{v_s}{\omega \cdot \varepsilon}, \qquad (7)$$

where v_s is sound velocity. Equation 7 shows that AlN is the champion at high frequency, where precision of lithography becomes the critical issue. At low frequencies, however, materials with low sound velocity and high dielectric constant appear to be better suited as they avoid too thick films and too large areas. In a ferroelectric, the ratio vs/ε is up to a factor of 200 smaller. Furthermore, many ferroelectrics exhibit larger coupling factors than AlN, and thus could allow for larger bandwidths or larger production tolerances. Finally, the polarization in ferroelectrics and paraelectrics can be changed by a superimposed DC electric field. The coupling coefficient can thus be varied within some limits, which could be attractive for tunable resonators [39, 40].

Ferroelectric TFBARs were explored in a number of works [28, 39, 41–43]. Despite large coupling constants k_t^2 of up to 25%, the figure of merit $k_t^2 Q$ was always very limited and did not exceed a value of 20. The main problem is the low quality factor that is commonly achieved. An attractive feature is the large possible bandwidth; even more attractive is the tuning capability.

Tuning is achieved by means of a DC electric field that is superimposed on the RF signal. A frequency shift of about 3% is obtained with a single-polarity DC field. A hysteresis loop of k_t^2 is shown in Fig. 8.

The quality factor problem is related to ferroelastic domains. The ferroelectric phase transition is usually accompanied by a distortion of the lattice. This distortion is defined in relation to polarization direction. In the case of uniaxial materials, the polarization direction is along the unique

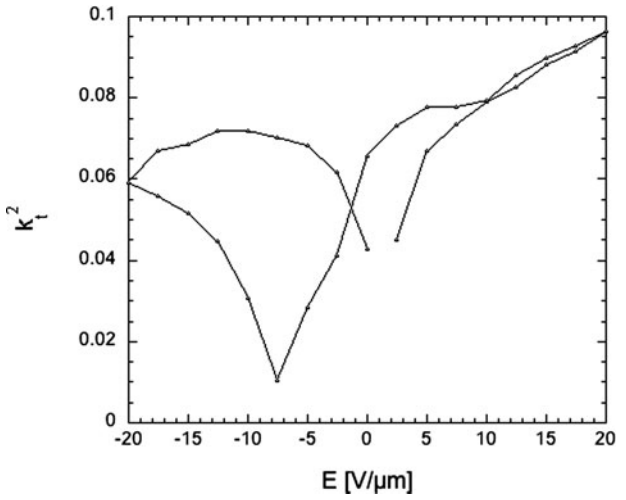

Fig. 8. TFBAR based on a 2 μm thick sol–gel PZT thin film resonating at 800 MHz. The coupling constant is shown as a function of a DC field applied to the resonator (from ref. [44]).

axis (*c*-axis), which is already defined in the para-electric phase. Hence, in a (001)-oriented film, the polarization is everywhere perpendicular to the film plane, and in the worst case ferroelectric strain causes homogeneous stress in the film (we obtain the same situation as in AlN). In materials without a unique axis, such as the perovskites, polarization may point along several directions. Considering the cubic–tetragonal transition, polarization may point along the $[001]_c$, $[100]_c$, and $[010]_c$ directions, where the index *c* indicates cubic notation. A purely random distribution of directions thus yields polarization only 1/3 perpendicular to the film plane if a (100)-oriented film was grown in the cubic phase. Reality is more complicated because the ferroelectric strains are different along the polarization direction than perpendicular to it. The resulting pattern of ferroelastic domains is governed by a thermodynamically driven equilibrium for diminishing elastic energy at a given overall strain dictated by the substrate. This phenomenon is well investigated in theory and experiment, and the reader is referred to the corresponding literature [45–48].

Most important in true ferroelectrics are phenomena related to domain wall motions and oscillations. It is known that the piezoelectric properties of morphotropic PZT ceramics are enhanced by domain wall displacements between ferroelastic domains by more than a factor of 2 [49]. Such information was obtained by freezing-in domain walls at cryogenic temperatures. Compatible to this picture is the observation that relaxations due to domain wall motions are observed at high frequencies in PZT and $BaTiO_3$, typically of the order of 1 to a few GHz (see review in [50, 51]). Figure 9 shows schematically the behavior of the permittivity of a piezoelectric resonator with domains (ceramics). At low frequencies the piezoelectric body can move freely. For a thin-film BAW, the only freedom is in the third dimension perpendicular to the film plane. At some given frequency, resonances occur defined by the geometry and dimensions of the body. At even higher frequencies, the mentioned relaxation is observed and permittivity drops by $\Delta\varepsilon$. The effect was explained by the ultrasonic emission of shear waves excited by domain wall oscillation, leading to a dielectric response of the form [51]:

$$\varepsilon_{tot} = \varepsilon_\infty + \frac{\Delta\varepsilon}{1 + i\omega\tau}. \tag{8}$$

As in the case of shape resonances, relaxation can be understood as resulting from trapped waves inside the domains. Waves are partially reflected at domain walls due to the orientation

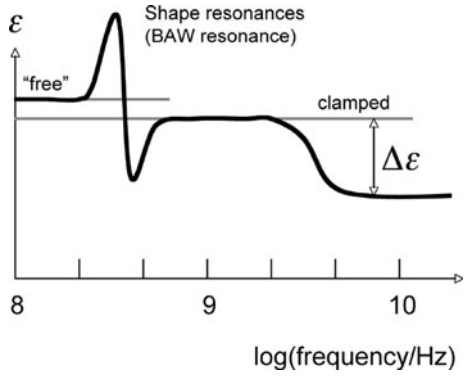

Fig. 9. Permittivity ε of a piezoelectric ceramic resonator (after [50]).

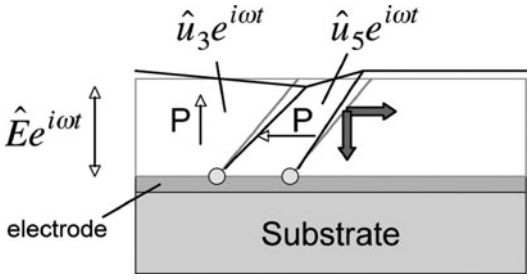

Fig. 10. Schematic drawing of 90° domain within *c*-axis-oriented tetragonal ferroelectric film.

dependence of acoustic impedance. The relaxation time thus depends on shear wave velocity v_{sh} and domain width *d* [51]:

$$\tau = \frac{d}{2v_{sh}}. \tag{9}$$

The situation for a tetragonal film is schematically sketched in Fig. 10. The electric field perpendicular to the film plane excites the longitudinal wave through piezoelectric strains or stresses as defined by the equation of state of the c-domain: $T_3 = e_{33}E_3$. In the 90° domain, however, the external electric field goes along the 1-axis of the local crystal system, and a shear stress $T_5 = e_{15}E_1$ is created. As a consequence, domain walls are displaced. Because the piezoelectric film is clamped on the substrate (electrode), the domain walls are most likely well fixed at the bottom; however, they can move further up. The moving domain walls lead to acoustic emission of shear waves running in all directions. Dissipation occurs due to the relaxation term in equation 8, and also due to waves dispersed laterally in the structure. The 90° domain width is normally much thinner than the film. Nevertheless, BAW resonance (=shape resonance) and domain wall resonances are expected to lie within the same frequency decade. This is even more the case because the shear velocity is smaller than the longitudinal one.

Thus it is important to control ferroelastic domains. Ideally, ferroelastic domains are avoided by using a substrate with large thermal expansion. In order to have small hysteresis, it is important to fix polarization well by a suitable poling process, and film composition. It is ideal to dispose of a material with no domain walls at all, as a monodomain ferroelectric, or alternatively a paraelectric such as $SrBaTiO_3$. In such material the losses are expected to be smaller. Currently, a great deal of research is ongoing to advance this paraelectric TFBAR [40, 52, 53].

VI. CONCLUSIONS

Some issues in process-property assessment for piezoelectric materials in microwave applications have been presented. It was shown that conclusive property assessment has to include acoustic test devices, combined with mathematical modeling. The frequently applied AlN thin films still bear some secrets related to precise mechanisms in polar growth. It looks as if still better properties can be expected, at least if it is possible to improve microstructure quality. Ferroelectric films look very attractive for tunable devices, applications below 1 GHz, and wide band filters. Their major handicap involves ferroelastic

domains, which lead to increased acoustic losses. For this reason, paraelectric materials with no domains look much more attractive. In any case, the control of ferroelectric domains is the key to applications of ferroelectric materials.

ACKNOWLEDGEMENTS

This work was supported by the Swiss Office for Education and Research in the frame of several European projects, and by the Swiss Commission of Innovation and Technology and the Swiss National Science Foundation (Grant no. 200021–112204). Micromachining work was performed at the Microtechnology Center CMI of EPFL. The TEM investigations were carried out at CIME-EPFL.

REFERENCES

[1] Hickernell, F.S.: ZnO processing for bulk- and surface wave devices, in IEEE Ultrasonics Symp., IEEE, Boston, MA, 1980, 785–794.

[2] Khuri-Yakub, B.T.; Kino, G.S.; Galle, P.: Studies of the optimum conditions for growth of rf-sputtered ZnO films. J. Appl. Phys., **46** (1975), 2464–2470.

[3] Yamamoto, T.; Shiosaki, T.; Kawabata, A.: Characterization of ZnO piezoelectric films prepared by rf planar magnetron sputtering. J. Appl. Phys., **51** (1980), 3113–3120.

[4] Shiosaki, T.; Ohnishi, S.; Kirokawa, Y.; Kawabata, A.: As grown CVD ZnO optical waveguides on sapphire. Appl. Phys. Lett., **33** (1978), 406–407.

[5] Grudkowski, T.W.; Black, J.F.; Reeder, T.M.; Cullen, D.E.; Wagner, R.A.: Fundamental-mode VHF-UHF miniature acoustic resonators and filters on silicon. Appl. Phys. Lett., **37** (1980), 993–995.

[6] Lakin, K.M.; Wang, J.S.: UHF composite bulk acoustic wave resonators, in IEEE Ultrasonics Symp., IEEE, Boston, 1980, 834–837.

[7] Nakamura, K.; Sasaki, H.; Shimizu, H.: ZnO/SiO_2-diaphragm composite resonator on a silicon wafer. Electron. Lett., **17** (1981), 507–509.

[8] Lakin, K.M.; Kline, G.R.; McCarron, K.T.: Thin film bulk acoustic wave filter for GPS, in IEEE Ultrasonics Symp., IEEE, 1992, 471–476.

[9] Lakin, K.M.; McCarron, K.T.; Rose, R.E.: Solidly mounted resonators and filters, in IEEE Ultrasonics Symp., IEEE, Seattle, 1995, 905–908.

[10] Ruby, R.C.; Bradley, P.; Oshmyansky, Y.; Chien, A.; Larson, J.D.: Thin film bulk acoustic wave resonators for wireless applications, in IEEE Ultrasonics Symp., IEEE, Atlanta, 2001, 813–821.

[11] Aigner, R.; Kaitila, J.; Ellia, J.; Elbrecht, L.; Nessler, W.; Handmann, M.; Herzog, T.; Marksteiner, S.: Bulk-acoustic wave filters: performance optimization and volume manufacturing, in IMS' 2003, Philadelphia.

[12] Heinze, H.; Schmidhammer, E.; Diekmann, C.; Metzger, T.: 3.8 × 3.8 mm^2 PCS-CDMA duplex incorporating thin film resonator technology, in IEEE Ultrasonics Symp., Montreal, 2004.

[13] Cushman, D.; Lau, K.F.; Garber, E.M.; Mai, K.A.; Oki, A.K.; Kobayashi, K.W.: SBAR filter monlithically integrated with HBT amplifier, in IEEE Ultrasonics, IEEE, Honolulu, USA, 1990, 519–523.

[14] Dubois, M.-A.; Carpentier, J.-F.; Vincent, P.; Billard, C.; Parat, G.; Muller, C.; Ancey, P.; Conti, P.: Monolithic above-IC resonators technology for integrated architectures in mobile and wireless communication. IEEE J. Solid-State Circuits, **41** (2006), 7–16.

[15] Ikeda, T.: Fundamentals of Piezoelectricity, Oxford University Press, Oxford, 1990.

[16] Masson, J.; Martin, G.; Boudot, S.; Gruson, Y.; Ballendras, S.; Artieda, A.; Muralt, P.; Belgacem, B.; Chomemeloux, L.: Fabrication of high stability oscillators using AlN/Si high overtone bulk acoustic resonators, in IEEE Ultrasonics Symp., IEEEE, New York, 2007, 628–631.

[17] Artieda, A.; Muralt, P.: High-Q AlN/SiO_2 symmetric composite thin film bulk acoustic wave resonators. IEEE Trans. UFFC., **55** (2008), 2463–2468.

[18] Ballato, A.; Gualtieri, J.G.: Advances in high-Q piezoelectric resonator materials and devices. IEEE Trans. UFFC., **41** (1994), 834–844.

[19] Gualtieri, J.G.; Kosinski, J.A.; Ballato, A.: Piezoelectric materials for acoustic wave applications. IEEE Trans. UFFC., **41** (1994), 53–59.

[20] Bu, G.; Ciplys, D.; Shur, M.; Schowalter, L.J.; Schujman, S.; Gaska, R.: Electromechanical coupling coefficient for surface acoustic waves in single-crystal bulk aluminum nitride. Appl. Phys. Lett., **84** (2004), 4611–4613.

[21] Tsubouchi, K.; Mikoshiba, N.: Zero-temperature coefficient SAW devices on AlN epitaxial films. IEEE Trans. Sonics Ultrason., **SU-32** (1985), 634–644.

[22] Martin, F.; Muralt, P.; Dubois, M.-A.; Pezous, A.: Thickness dependence of properties of highly *c*-axis textured AlN thin films. J. Vac. Sci. Technol. A., **22** (2004), 361–365.

[23] Kamiya, T.: Calculation of crystal structures, dielectric constants and piezoelectric properties of Wurtzite-type crystals using ab-intio periodic Hartree–Fock method. Jpn. J. Appl. Phys., **41** (1996), 4421–4426.

[24] Löbl, H.P.; Klee, M.; Metzmacher, C.; Brand, W.; Milsom, R.; Lok, P.: Piezoelectric thin AlN films for bulk acoustic wave resonators. Mater. Chem. Phys., **79** (2003), 143–146.

[25] Tsubouchi, K.; Sugai, K.; Mikoshiba, N.: AlN material constants evaluation and SAW properties of AlN/$Al2O_3$ and AlN/Si, in IEEE Ultrasonics Symp., 1981, 375–380.

[26] Tornare, G.; Calame, F.; Muralt, P.: unpublished.

[27] Dubois, M.-A.; Muralt, P.: Stress and piezoelectric properties of AlN thin films deposited onto metal electrodes by pulsed direct current reactive sputtering. J. Appl. Phys., **89** (2001), 6389–6395.

[28] Takikawa, H.; Kuimura, K.; Miyano, R.; Sakakibara, T.; Bendavid, A.; Martin, P.J.; Matsumuro, A.; Tsutsumi, K.: Effect of substrate bias on AlN thin film preparation in shielded reactive vacuum arc deposition. Thin Solid Films, **386** (2001), 276–280.

[29] Drusedau, T.P.; Blasing, J.: Optical and structural properties of highly *c*-axis oriented nitride prepared by sputter deposition in pure nitride. Thin Solid Films, **377** (2000), 27–31.

[30] Gardeniers, J.G.E.; Rittersma, Z.M.; Burger, G.J.: Preferred orientation and piezoelectricity in sputtered ZnO films. J. Appl. Phys., **83** (1998), 7844–7854.

[31] Bjurstrom, J.; Rosen, D.; Katardjiev, I.; Yanchev, V.M.; Petrov, I.: Dependence of the electromechanical coupling on the degree of orientation of c-texture thin AlN films. IEEE Trans. UFFC., **51** (2004), 1347–1353.

[32] Link, M.; Schreiter, M.; Weber, J.; Gabl, R.; Pitzer, D.; Primig, R.; Wersing, W.; Assouar, M.B.; Elmazria, O.: *C*-axis inclined ZnO films for shear-wave transducers deposited by reactive sputtering using an additional blind. J. Vac. Sci. Technol. A., **24** (2006), 218–222.

[33] Bjurstrom, J.; Wingqvist, G.; Katardjiev, I.: Synthesis of textured thin film piezoelectric AlN films with a nonzero *c*-axis mean tilt for the fabrication of shear mode resonators. IEEE Trans. UFFC., **53** (2006), 2095–2100.

[34] Warren, B.E.: X-ray Diffraction, Addison-Wesley, Reading, MA, 1969.

[35] Vogg, G.; Miskys, C.R.; Garrido, J.A.; Herman, M.; Eickhoff, M.; Stutzmann, M.: High quality heteroepitaxial AlN films on diamond. J. Appl. Phys., **96** (2004), 895–902.

[36] Ruffner, J.A.; Clem, P.G.; Tuttle, B.A.; Dimos, D.; Gonzales, D.M.: Effect of substrate composition on the piezoelectric response of reactively sputtered AlN thin films. Thin Solid Films, **354** (1999), 256–261.

[37] Lakin, K.M.; Kline, G.R.; McCarron, K.T.: High-Q microwave acoustic resonators and filters. IEEE Trans. Microwave Theory Tech., **41** (1993), 2139–2146.

[38] Martin, J.J.: Acoustic loss in cultured quartz, in IEEE International Frequency Control Symp., 1996, 170–178.

[39] Schreiter, M.; Gabl, R.; Pitzer, D.; Wersing, W.: Electro-acoustic hysteresis behavior of PZT thin film bulk acoustic resonators. J. Eur. Cer. Soc., **24** (2004), 1589–1592.

[40] Gevorgian, S.; Vorobiev, A.; Lewin, T.: DC field and temperature dependent acoustic resonances in parallel-plate capacitors based in $SrTiO_3$ and (Ba,Sr)TiO_3 films: experiment and modelling. J. Appl. Phys., **99** (2006), 124112.

[41] Löbl, H.P.; Klee, M.; Milsom, R.; Dekker, R.; Metzmacher, C.; Brand, W.; Lok, P.: Materials for bulk acoustic wave (BAW) resonators and filters. J. Eur. Cer. Soc., **21** (2001), 2633–2640.

[42] Larson, J.D.; Gilbert, S.R.; Xu, B.: PZT material properties at UHF and microwave frequencies derived from FBAR measurements, in IEEE Ultrasonics Symp., Montreal, 2004.

[43] Su, Q.X.; Kirby, P.; Komuro, E.; Imura, M.; Zhang, H.; Whatmore, R.W.: Thin film bulk acoustic resonators and filters using ZnO and PZT thin films. IEEE Trans., **MTT 49** (2001), 769–777.

[44] Conde, J.; Muralt, P.: Characterization of sol–gel PZT thin film bulk acoustic resonators. IEEE Trans. UFFC., **55** (2008), 1373–1379.

[45] Roitburd, A.L.: Equilibrium structure of epitaxial layers. Phys. Status Solidi (a), **37** (1976), 329–339.

[46] Roytburd, A.L.: Thermodynamics of polydomain heterostructures. I. Effect of macrostresses. J. Appl. Phys., **83** (1998), 228–238.

[47] Speck, J.S.; Pompe, W.: Domain configurations due to multiple misfit relaxation mechanisms in epitaxial ferroelectric films I. Theory. J. Appl. Phys., **76** (1994), 466–476.

[48] Pertsev, N.A.; Zembilgotov, A.G.; Tagantsev, A.K.: Effect of mechanical boundary conditions on phase diagrams of epitaxial ferroelectric thin films. Phys. Rev. Lett., **80** (1998), 1988–1991.

[49] Zhang, Q.M.; Wang, H.; Kim, N.; Cross, L.E.: Direct evaluation of domain-wall and intrinsic contributions to the dielectric and piezoelectric response and their temperature dependence on lead zirconate–titanate ceramics. J. Appl. Phys., **75** (1994), 454–459.

[50] Arlt, G.: Strong ultrasonic microwaves in ferroelectric ceramics. IEEE Trans. UFFC., **45** (1998), 4–10.

[51] Arlt, G.; Böttger, U.; Witte, S.: Emission of GHz shear waves by ferroelastic domain walls in ferroelectrics. Appl. Phys. Lett., **63** (1993), 602–604.

[52] Noeth, A.; Yamada, T.; Sherman, V.O.; Muralt, P.; Tagantsev, A.; Setter, N.: DC Bias-dependent shift of the resonance frequencies in BST thin film membranes. IEEE Trans. UFFC., **54** (2007), 2488–2492.

[53] Volatier, A.; Defay, E.; Aid, M.: Switchable and tunable strontium electrostrictive bulk acoustic wave resonator integrated with a Bragg mirror. Appl. Phys. Lett., **92** (2008), no. 032906.

Paul Muralt is a professor in materials science, and group leader for thin film and MEMS activities at the Ceramics Laboratory, both of the Swiss Federal Institute of Technology EPFL, at Lausanne, Switzerland. He holds a diploma in experimental physics and a Ph.D. degree from the Swiss Federal Institute of Technology ETH in Zurich. At the IBM Research Laboratory in Zurich, he pioneered the application of scanning tunneling microscopy to electrical potential imaging (1985). In 1987 he joined the Balzers group in Liechtenstein, becoming manager for development and applications of thin-film deposition processes. In 1993, he joined EPFL, where he started activities in ferroelectric thin films and MEMS devices. His interests are in thin-film growth, integration, and properties of functional oxide materials. More recent works deal with the fabrication and study of ferroelectric nano-structures, and oxygen ion conductors for micro-solid oxide fuel cells. As a teacher, he gives lectures in thin-film deposition, micro-patterning, and ceramics. He has authored and co-authored more than 200 scientific articles.

Janine Conde was born in South Shields, England, on May 26, 1979. She received her M.S. degree in materials science from the Swiss Federal Institute of Technology in Zurich (ETHZ), Switzerland, in 2004. Since 2004 she is a Ph.D. student and research assistant at the Institute of Material Science at EPFL.

Alvaro Artieda was born in Lima, Peru, in 1978. He received a Master of Science in Physics in 2005 at the Ecole Polytechnique Federale de Lausanne (EPFL), Switzerland. In 2006 he joined the Ceramics Laboratory of the EPFL as a Ph.D. student. His research interest is focused in the field of micro-electro-mechanical devices (MEMS) and thin-film deposition and properties. He specializes in properties and applications of piezoelectric materials such as aluminum nitride (AlN). The specific target of his work is to study new thin-film structures for high-Q resonators in integrated oscillators and sensors.

Fabrice Martin was born in 1972. He received a B.Sc. (Hons) degree in applied physics in 1996 and a Ph.D. degree in 2003 from The Nottingham Trent University in the field of acoustic wave sensors. He joined the Ceramics Laboratory at the Ecole Polytechnique Fédérale de Lausanne, EPFL, Switzerland, as a research fellow from 2002 to 2006, where he specialized in piezoelectric and ferroelectric thin-film technology.

Marco Cantoni was born in 1963 in Schaffhausen, Switzerland. He graduated 1994 at ETHZ in Experimental Physics. He joined the electron microscopy center (CIME) at EPFL 1998 after a 2 years stay in Japan at the National Institute for Reasearch in Inorganic Materials (NIRIM) in Tsukuba. From 2001 to 2005 he was in the ceramics laboratory LC at EPFL with a focus on ferroelectric relaxor materials providing also advanced TEM service to the whole laboratory. Since 2006 he is in the electron microscopy center responsible for advanced TEM and analytical techniques. As the EM-facility manager for basic science and materials science he is giving lectures about electron microscopy and he is also responsible for the user training.